Original Article

Induction of Apoptosis in Hormone-resistant Human Prostate Cancer PC3 Cells by Inactivated Sendai Virus[*]

GAO Hui[1], GONG Xiao Cheng[2], CHEN Ze Dong[1], XU Xiao Shuang[2],
ZHANG Quan[2,#], and XU Xiang Ming[2,3,#]

1. College of Clinical Medicine of Yangzhou University, Yangzhou 225001, Jiangsu, China; 2. Jiangsu Co-innovation Center for Prevention and Control of Important Animal Infectious Diseases and Zoonoses, Yangzhou University, Yangzhou 225009, Jiangsu, China; 3. Suzhou Polytechnic Institute of Agriculture, Suzhou 225008, Jiangsu, China

Abstract

Objective   Inactivated Sendai virus particle [hemagglutinating virus of Japan envelope (HVJ-E)] has a potential oncolytic effect due to its ability to induce apoptosis in tumor cells. However, the molecular mechanism of apoptosis induction in cancer cells mediated by HVJ-E has not been fully elucidated. This paper aims to investigate the underlying mechanism of apoptosis induction by HVJ-E in prostate cancer cells (PC3).

Methods   PC3 cells were treated with HVJ-E at various MOI, and then interferon-β (IFN-β) production, and the cell viability and apoptosis were detected by ELISA, MTT-based assay and flow cytometry, respectively. Next, the roles of Jak-Stat, MAPK and Akt pathways played in HVJ-E-induced apoptosis in PC3 cells were analyzed by immunoblot assay. To further evaluate the cytotoxic effect of HVJ-E on PC3 cells, HVJ-E was intratumorally injected into prostate cancers on BALB/c-nude mice, and the tumor volume was monitored for 36 days.

Results   HVJ-E induced IFN-β production and activated Jak-Stat signaling pathway, which resulted in the activation of caspase-8, caspase-3, and PARP in PC3 prostate cancer cells post HVJ-E treatment. Furthermore, we observed for the first time that p38 and Jnk MAPKs in PC3 cells contributed to HVJ-E-induced apoptosis. In addition, intratumoral HVJ-E treatment displayed a direct inhibitory effect in an *in vivo* BALB/c nude mouse prostate cancer model.

Conclusion   Our findings have provided novel insights into the underlying mechanisms by which HVJ-E induces apoptosis in tumor cells.

Key words: Inactivated Sendai virus (HVJ-E); Apoptosis; Caspase; Mitogen-activated protein kinase (MAPK)

INTRODUCTION

Prostate cancer is one of the most common solid tumors in men and one of the major leading causes of cancer-related deaths worldwide[1]. Prostate cancer cells in patients initially respond to androgen withdrawal therapy by undergoing apoptosis, but then the apoptosis-resistant cells survive and develop into androgen-refractory phenotype[2]. Androgen-refractory

prostate cancer is more resistant to a number of therapeutic modalities, including chemotherapy and radiotherapy, and is ultimately lethal[3]. Therefore, there is an urgent need for novel treatment strategies for androgen-refractory prostate cancers.

In recent years, great stride has been made in cancer virotherapy following the development of oncolytic viruses, which enables viruses to replicate in cancer cells selectively[4]. The New Castle disease virus (NDV) virulent strain (FMW), mesogenic strains (73-T, MTH-68/H, and PV701) and lentogenic strains (HUJ and Ulster) have been used for cancer treatment[5-8]. However, the oncolytic efficacy is low due to the suppression of the virus by host immune responses. Furthermore, the oncolytic activity is lost following UV irradiation[9].

Inactivated Sendai virus particle (hemagglutinating virus of Japan envelope, HVJ-E) obtained via UV irradiation was found to display effective oncolytic activity without replication ability[10]. UV-inactivated Sendai virus generates antitumor immunity via both activation of CTL, natural killer (NK) cells and suppression of regulatory T cells[11-13]. Furthermore, HVJ-E induces apoptosis in castration-resistant human prostate cancer cells without any toxic effects on nonmalignant prostate epithelial cells[3,14]. However, the molecular mechanism of apoptosis induction in cancer cells mediated by HVJ-E has not been fully elucidated.

In this study, in addition to Jak/Stat signaling pathway, we demonstrate for the first time that p38 and Jnk mitogen-activated protein kinase (MAPK) pathways are involved in apoptosis in HVJ-E-treated PC3 cells. Our findings provide novel insights into the underlying mechanisms by which HVJ-E induces apoptosis in cancer cells.

MATERIALS AND METHODS

Cells and Virus

Hormone-resistant human prostate cancer cell PC3, hormone-sensitive human prostate cancer cell LNCap clone FGC and human normal prostatic epithelial cell, RWPE-1 were purchased from the Cell Bank of the Chinese Academy of Science (Shanghai, China). The cells were cultured in RPMI 1640 medium supplemented with 10% fetal bovine serum (FBS). Sendai virus (Z strain) was used throughout the study. Sendai virus was purified from the chorioallantoic fluid from 10 to 14 day-old chick eggs, after which it was purified by centrifugation and

inactivated by UV irradiation (99 mJ/cm^2), as previously described[15].

Antibodies and Reagents

The following antibodies from Cell Signaling Technology (Beverly, MA) were used: caspase-3, caspase-8, caspase-9, Cytochrome c, phospho-Jnk, phospho-p38, phospho-Akt, phospho-Stat1, total p38, total Akt, RIG-I, the poly (ADP-ribose) polymerase (PARP), and β-actin. Specific inhibitors of Jnk (SP600125), and p38 (SB2035801) were purchased from Cell Signaling Technology (Beverly, MA). Horseradish peroxidase-conjugated goat anti-rabbit immunoglobulin, propidium iodide (PI) and Hoechst 33258 were from Sigma-Aldrich (Shanghai, China). Jak inhibitor I was purchased from Santa Cruz Biotechnology (Santa Cruz, CA). FITC Annexin V Apoptosis Detection Kit I was purchased from BD Biosciences (San Diego, CA).

Cell Viability Assay

Cell viability was determined using the MTT assay based on the formation of formazan crystals from tetrazolium by living cells. MTT assay was performed as previously described[16]. The experiments were repeated for three times.

Flow Cytometry Analysis of Apoptosis

Apoptosis was determined by flow cytometric analysis of membrane redistribution of phosphatidylserine using an annexin V and propidiu iodide (PI) double staining technique. The experiment was performed as described elsewhere. A total of 20 000 PC3 cells were either mock treated or treated with HVJ-E at a MOI of 100, 400, and 600. The percentage of apoptotic cells was determined in three independent experiments. For the apoptosis inhibition assay, PC3 cells were incubated with Jak inhibitor I (5 μmol/L), SP60025 (20 μmol/L), or SB203580 (10 μmol/L) for 3 h prior to treatment with HVJ-E. The treated cells were monitored for apoptosis at 400 MOI of HVJ-E.

Hoechst 33258 Staining

Apoptotic nuclear changes were examined using Hoechst 33258 staining. The cells were fixed with 4% paraformaldehyde, stained with Hoechst 33258 (5 μg/mL) for 10 min and examined under a fluorescence microscopy to analyze cell chromatin condensation.

Immunoblot Assay

PC3 cell plated in 60-mm dishes were treated with HVJ-E at different MOI. Twenty four hours later, the treated cells were harvested and lysed, and an immunoblot (IB) assay was performed as described previously[17]. All IB experiments were performed twice.

In vivo Oncolysis

Twenty 6-week-old BALB/c-nude mice were randomly divided into 2 groups, where each group contained 5 female and 5 male mice. Viable PC3 cells (2×10^6 cells) were intradermally injected into the backs of the mice. When each inoculated tumor reached 4-6 mm in diameter, HVJ-E (1.5×10^{10} particles in a total volume of 100 µL) or PBS was injected into tumors on days 12, 15, and 18. Tumor volume was measured in a blinded manner with slide calipers using the following formula: tumor volume (mm^3) = length × $(width)^2$/2.

Statistical Analysis

For all experiments, the statistical analysis was performed for all groups using a one-way analysis of ANOVA to determine statistical significant variance between the groups for each endpoint assessed. Differences with a P value <0.05 were considered statistically significant.

RESULTS

HVJ-E Activates RIG-I Expression and Induces IFN-β Production in PC3 Cells

RIG-I functions as a virus sensor in a certain type of cells, such as macrophages, fibroblast and conventional dendritic cells (cDC), which use RIG-I like receptor system for the antiviral activity[18]. Synthesized RNA can be a ligand for RIG-I as well as native viral RNA[19]. HVJ-E contains single-stranded RNA fragments of approximately 300 bp, which can be recognized by RIG-I in human cancer cells[10]. To investigate whether HVJ-E activates RIG-I expression in PC3 cells and induces type I IFN production, PC3 cells were treated with HVJ-E at different MOI, at 24-h post-treatment, and cell lysate and cell supernatant were then harvested for RIG-I detection and IFN-β determination. As shown in Figure 1A, the expression of RIG-I was augmented upon HVJ-E treatment in a dose dependent manner, indicating that HVJ-E fused effectively with PC3 cells and the broken viral genomes were recognized by RIG-I, which resulted in an increasing amount of IFN-β production in PC3 cells with the increment of HVJ-E (Figure 1B).

HVJ-E Induces Apoptosis in PC3 Cells

IFN-β is able to induce cell death in numerous human cancer cell lines[20-21]. In the present study, HVJ-E was demonstrated to have the ability to elicit IFN-β production in PC3 cells. Therefore, the effects of HVJ-E on the proliferation and viability of PC3 cells were examined. PC3 cells treated with HVJ-E from 50 to 1000 MOI for 24 h were shown to lead to a dose-dependent reduction in cell viability as compared to controls (Figure 2A). However, growth inhibition of hormone sensitive LNCap cell and normal prostate epithelium was not observed, and these results have been confirmed by others that the amount of receptors for HVJ, GD1a, and SPG, are much higher in PC3 cells than hormone-sensitive prostate cancer
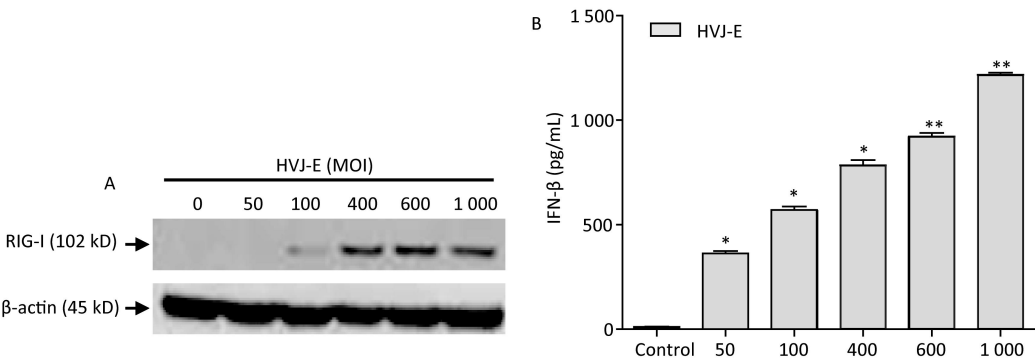

Figure 1. HVJ-E induces IFN-β production in PC3 cells. (A) PC3 cells were treated with HVJ-E at the indicated MOI for 24 h, and cell extracts were then assessed for RIG-I expression. (B) IFN-β production in PC3 cells treated with HVJ-E at indicated MOI. The data show the mean±SD of three experiments in quadruplicate. *P<0.05 or **P<0.01 compared with controls.

LNCap cells and normal prostate epithelium[14]. Next, we sought to examine whether the reduced proliferation and viability by HVJ-E were due to the apoptosis in PC3 cells. Flow cytometry assay was performed to analyze PC3 cells treated with HVJ-E at MOI of 100, 400, and 600 respectively. As shown in Figures 2B and 2C, PC3 cells in response to HVJ-E also resulted in remarkable apoptosis in a dose-dependant manner, indicating that an oncolytic effect was produced by HVJ-E in PC3 cells. Furthermore, the apoptotic effect induced by HVJ-E in PC3 cells was further assessed by fluorescence microscopy and microscopy observation. Apoptotic chromatin condensation and nuclear fragmentation were readily observed in HVJ-E-treated cells by Hoechst 33258 staining (Figure 2D). Meanwhile, compared
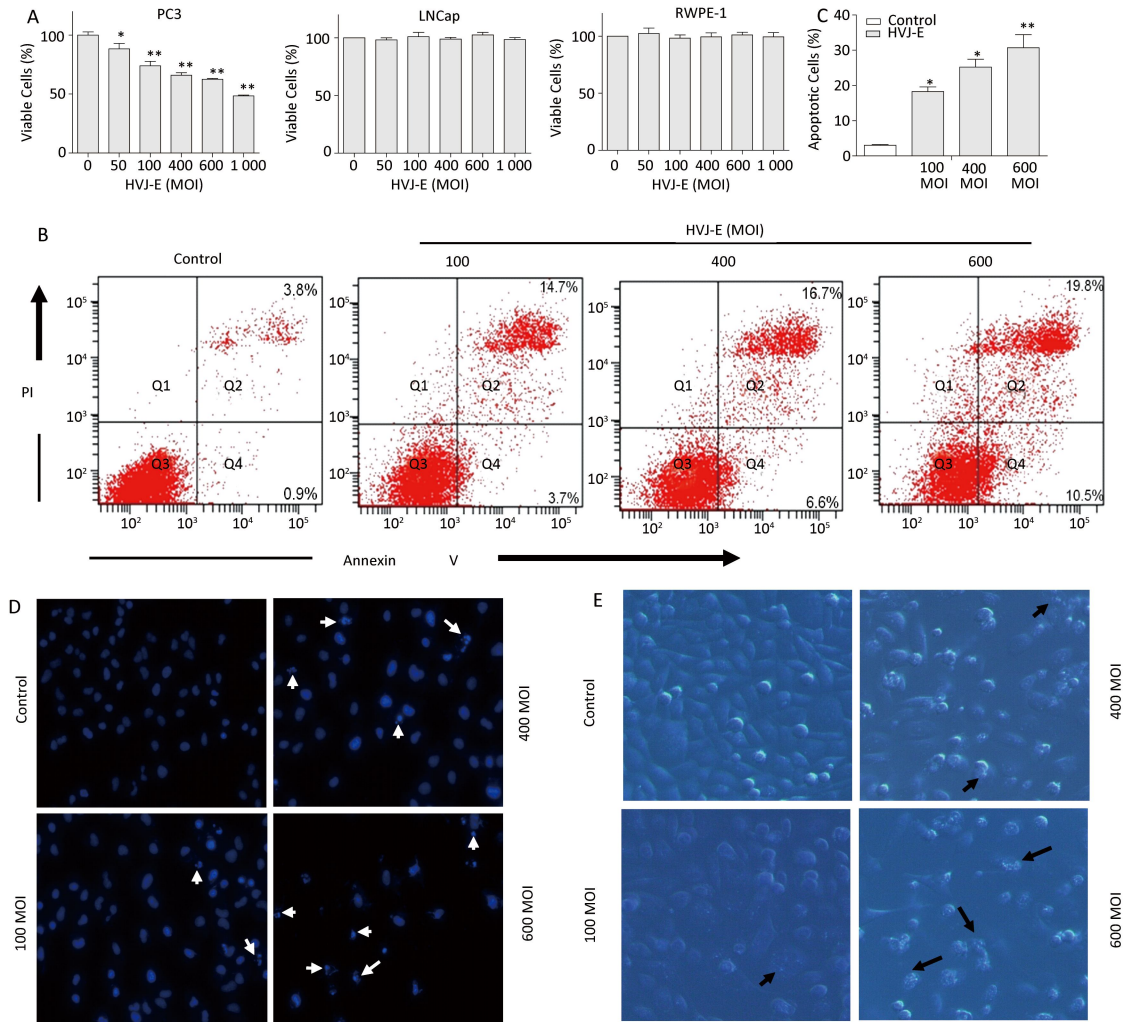

Figure 2. HVJ-E induces apoptosis in PC3 cells. (A) The effect of increasing MOI of HVJ-E on cell viability of PC3, LNCap and RWPE-1 cells was assessed by MTT-based assay. The data show the mean±SD of three experiments in quadruplicate. (B and C) PC3 cells were either mock- treated or treated with HVJ-E at MOI of 100, 400, and 600 for 24 h, the cells were harvested and double-stained with annexin V and propidium iodide (PI) and then analyzed by flow cytometry. The cell population in the right lower quadrant (PI-negative, Annexin V-positive) corresponded to early stage apoptotic cells; the right upper quadrant (Annexin V/PI positive) corresponded to late stage apoptotic and necrotic cells. A representative result from three independent experiments was shown. (D) PC3 cells were treated as described above, stained with Hoechst 33258 and cell morphology was analyzed by fluorescence microscopy (arrows, apoptotic cells, 200×). All experiments were performed twice. (E) Microscopic observation (400×) of PC3 cells 24 h post HVJ-E treatment. HVJ-E induced cell disintegration (arrows) and significantly reduced the number of viable cancer cells. *P<0.05 or **P<0.01 compared with controls.

with controls, HVJ-E treated cells not only represented the reduction of cell number but also represented shrinkage and cell disintegration (Figure 2E).

Jak-stat Pathway Plays Partial Role in HVJ-E Induced Apoptosis

Type I IFN was known to induce apoptosis in some transformed cell lines via Jak/stat pathway, and the activation of caspase pathway was mediated by the phosphorylation of Stat1[20-22]. Therefore, the activation of Stat1 and downstream caspases and PARP was assayed. As shown in Figure 3A, the phosphorylation of Stat1 was detected with HVJ-E at all indicated MOI, meanwhile, the cleavage of caspase-8, Cytochrome c, caspase-3, and PARP was
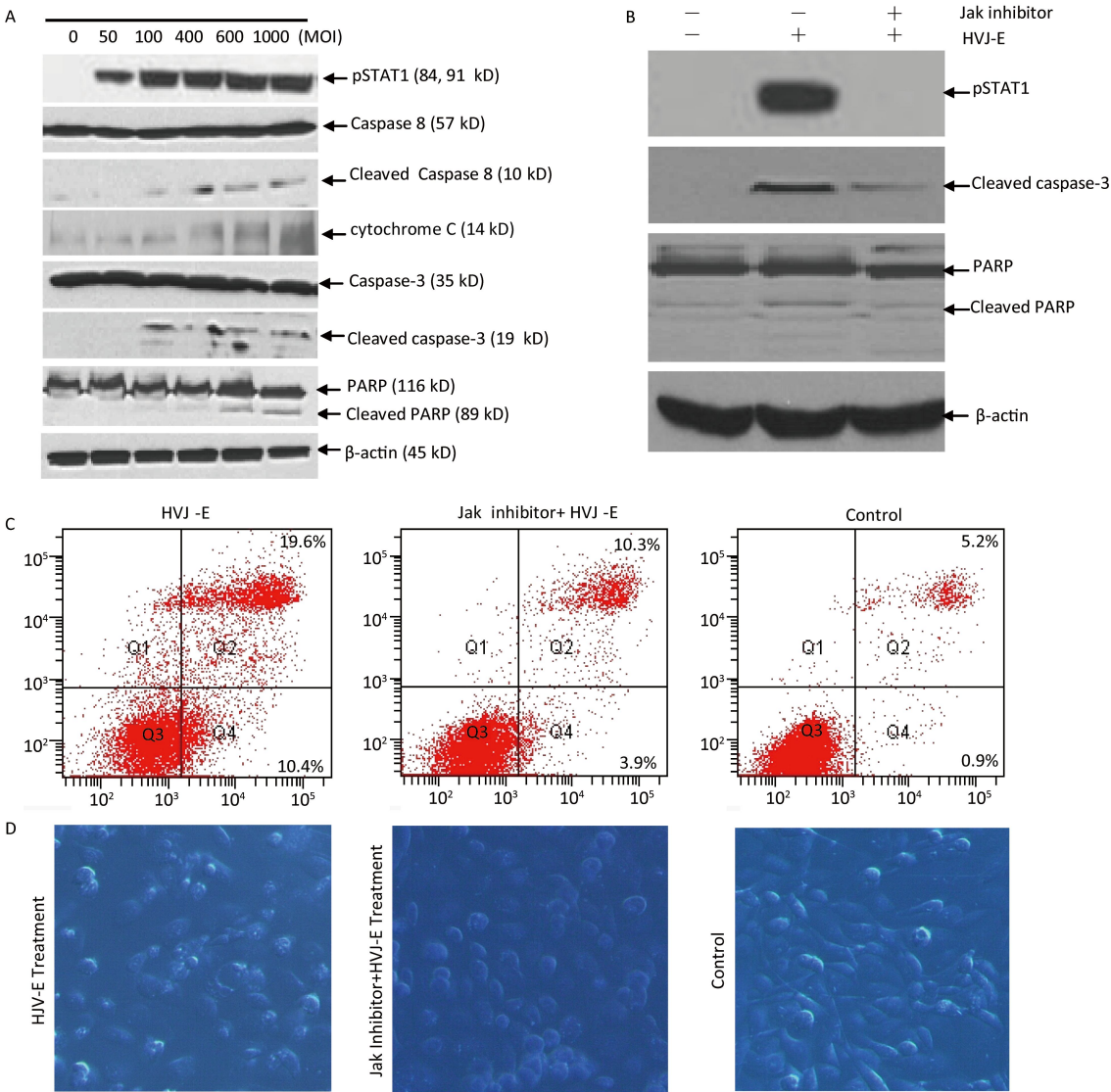

Figure 3. Jak-Stat pathway played a partially role in HVJ-E-induced PC3 cells apoptosis. PC3 cells were either mock-treated or treated with HVJ-E at indicated MOI. Cell lysates were analyzed by immunoblot (IB) assay with appropriate antibodies for the apoptotic pathway. (A) Detection of the activated forms of Stat1, caspase-8, Cytochrome c, caspase-3, and cleaved PARP. β-actin protein level was assessed for loading control. All IB experiments were carried out twice. (B) PC3 cells were either mock-treated or pretreated with a Jak inhibitor (5 μmol/L) before HVJ-E treatment (MOI=600), and then phospho-Stat1, cleaved caspase-3 and PARP were assayed by IB. (C) PC3 cells were either mock-treated or pretreated with Jak inhibitor (5 μmol/L) before HVJ-E treatment (MOI=600), and apoptotic cells were measured by flow cytometry. (D) PC3 cells were treated as above and cell morphology was observed under a microscope (400×).

also detected from 100 to 1000 MOI, however, the activated caspase-9 was undetectable (data not shown), indicating that the caspase pathway, especially extrinsic pathway may be involved in apoptotic induction by HVJ-E in PC3 cells.

To further confirm whether the apoptotic induction by HVJ-E in PC3 cells was Jak/Stat pathway dependent, cells were pretreated with Jak inhibitor, then the activation of Stat1 and cleavage of caspase-3 and PARP in HVJ-E-treated cell was determined, meanwhile, the treated cells were subjected to apoptotic analysis and microscopic observation. As shown in Figure 3B, pretreatment with Jak inhibitor for 3 h markedly suppressed the phosphorylation of Stat1 and the cleavage of caspase-3 and PARP. However, although pretreatment with Jak inhibitor obviously inhibited HVJ-E-induced apoptosis and significantly prevented cell disintegration (Figure 3C, 3D), the apoptosis induction by HVJ-E in PC3 cells were not completely blocked, which suggested that some other signaling pathways could also contribute to HVJ-E-induced apoptosis in PC3 cells.

MAPK Pathways Play roles in HVJ-E-induced Apoptosis in PC3 Cells

MAPK and Akt signaling pathways are well known to play important roles in regulation of cell proliferation and apoptosis in response to a variety of stimuli[23]. To investigate the regulation of MAPK and Akt pathways in HVJ-E-treated PC3 cells, phosphorylation of Erk1/2, Jnk, p38 MAPK and, Akt were detected by IB assay using appropriate antibodies. As illustrated in Figure 4A, p38 MAPK and Jnk were activated while the phosphorylation of Erk1/2 was undetectable (data not shown). In addition, the phosphorylation level of Akt in PC3 cells remains unchanged after HVJ-E treatment. Interestingly, the blockade with Jak inhibitor prior to HVJ-E treatment failed to inhibit the activation of p38 and Jnk MAPKs, further suggesting that p38 and Jnk MAPKs might contribute to HVJ-E-induced apoptosis (Figure 4B).

To further investigate the roles that MAPK pathways played in HVJ-E induced apoptosis in PC3 cells, specific inhibitors, SB203580 and SP600125, targeting p38 MAPK and JNK, respectively, were added to PC3 cells 30 min prior to HVJ-E treatment and cell viability was determined by MTT-based assay. The results showed that PC3 cell proliferation was not affected by treatment with the inhibitors at their specific concentration (10 μmol/L for SB203580 and 20 μmol/L for SP600125) (Figure 4C), and

inactivation of the target pathway by specific inhibitors was confirmed by IB assay (Figure 4D). As shown in Figure 4E, the two inhibitors exhibited significant inhibition of cytotoxicity at 24, 48, and 72 h post treatment ($P<0.05$ or $P<0.01$). Moreover, the microscopic observation and cell-cycle apoptosis detection also confirmed that the inhibitors could reduce the cytotoxic effect induced by HVJ-E on PC3 cells (Figure 4F). These results together suggest that JNK and p38 MAPK pathways contribute to HVJ-E induced apoptosis in PC3 cells.

HVJ-E Acts as an Effective Oncolytic Agent in a BALB/c-nude Mouse Prostate Cancer Model

To further evaluate the ability of HVJ-E to induce PC3 cell apoptosis *in vivo*, HVJ-E particles were injected into transplanted prostate cancer tumors when they reached about 5 mm in diameter for three times (day 12, 15, and 18). Then, tumor volume was detected and analyzed, and effective inhibition of prostate tumor growth in HVJ-E-injected BALB/c nude mice was demonstrated as compared with that in control mice (Figure 5), indicating that HVJ-E could directly induce apoptosis in B16F10 melanoma cells *in vivo* and delay tumor growth independent of any T cell-dependent cytotoxicity.

DISCUSSION

To date, there have been a number of reports describing oncolysis mediated by replication-ompetent viruses[4,6,24-26]. Replication is necessary for cancer cell killing induced by oncolytic viruses, and the oncolytic ability of these viruses is lost following UV inactivation[9]. However, UV-irradiated HVJ (HVJ-E) displays oncolytic activity without viral genome replication and viral protein synthesis. The antitumor activities of HVJ-E have been reported in previous publications[11,13,27-28]. These activities include the activation of antitumor immunity and induction of apoptosis. Although the mechanism of antitumor immunity activation has been extensively elucidated[11-12], the precise mechanism of HVJ-E-induced apoptosis has not been extensively examined.

A previous study has reported that RIG-I is the key cytosolic receptor responsible for the detection of the breaked viral RNA of HVJ-E and for type I IFN induction[10]. In the current study, the expression of RIG-I was increased with the increment of HVJ-E, and IFN-β was also produced in response to HVJ-E treatment in a dose-dependant manner, which was
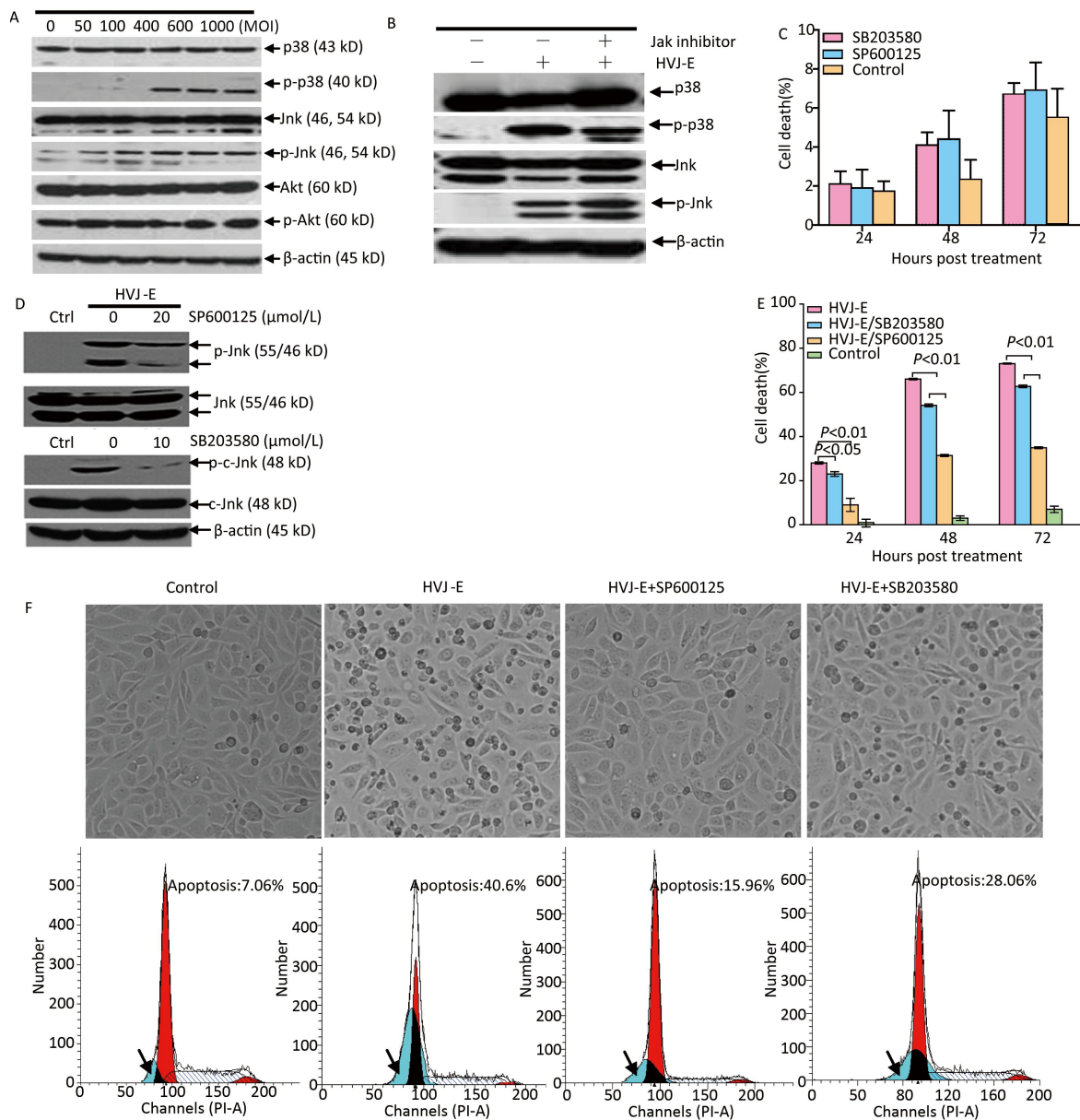
Figure 4. MAPK pathways contribute to HVJ-E treated apoptosis in PC3 cells. (A) PC3 cells were treated as above, and the regulation of MAPK and Akt pathways were examined with specific antibodies for activated Jnk, p38 MAPK and Akt. Total protein levels were assessed as a loading control. (B) PC3 cells were either mock-treated or pretreated with a Jak inhibitor (5 μmol/L) before HVJ-E treatment (MOI=600), and then phosphor-Jnk and phosphor-p38 were assayed by IB. (C) PC3 cells were either mock-treated or pretreated with SP600125 (20 μmol/L) or p38 inhibitor SB203580 (10 μmol/L) for 30 min. Cell viability was measured by MTT-based assay. Values were mean±SD from three independent experiments. (D) PC3 cells were pretreated with inhibitors at indicated concentrations. The cell lysates were prepared for IB assay to examine the inactivation of target pathways. (E) PC3 cells were either mock-treated or pretreated with indicated inhibitors for 30 min respectively, cells were then treated with HVJ-E at an MOI of 600 for indicated time points or sham-treated. Cell viability was then determined by the MTT assay. Data presented were mean±SD calculated from three independent experiments. (F) PC3 cells were treated as above and cell morphology (400×) and cell-cycled apoptosis were assayed.
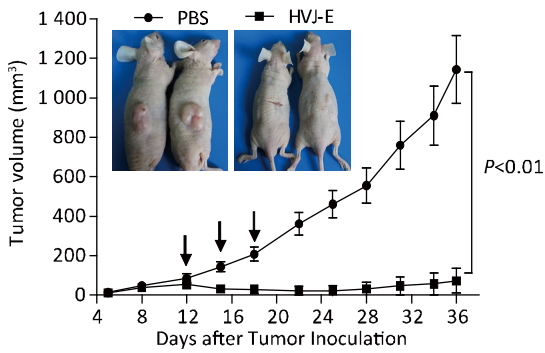
Figure 5. HVJ-E inhibited tumor growth on BALB/c nude mice. PC3 cells were inoculated into intradermal space in the backs of BALB/c-nude mice. Replication defective particles (1.5×10^{10} each) of HVJ-E or PBS were injected into tumors thrice (on day 12, 15, and 18). The HVJE-treated tumors were effectively inhibited as compared with PBS-treated tumors.

consistent with the previous report[14]. IFN-β-induced apoptosis was dependent on activation of the caspase cascade with cleavage of caspases 3, 8, and PARP[21], in addition, the activation of caspase pathway was regulated by the phosphorylation of Stat and Jak-Stat signal pathway[22], therefore, to examine whether the caspase pathway contributes to apoptosis induction in PC3 cells, the phosphorylation of Stat1 and the activation of caspase-8, caspase-9, caspase-3, and PARP in HVJ-E-treated PC3 cells was detected. The results revealed that stat1 and caspase-8, Cytochrome c, caspase-3 and PARP were activated upon HVJ-E treatment, while the activation of caspase-9 was undetectable, which was also in line with the previous report[14]. The pretreatment of Jak inhibitor effectively inhibited the phosphorylation of Stat and cleaved caspase-3 and PARP, however, the cell apoptosis and cell death were not completely blocked by use of Jak inhibitor, indicating other signaling pathways may be involved in apoptotic induction by HVJ-E in PC3 cells.

Although a recently published report has demonstrated that TNF-related apoptosis-inducing ligand (TRAIL) and Noxa represent promising target molecules for cancer cell-selective apoptosis when RIG-I/MAVS signaling pathway is activated in prostate cancer cells[3], to our knowledge, very few reports concerning the regulation of MAPK and Akt pathways in HVJ-E-induced cancer cell apoptosis have been presented. Here, we have for the first time provided evidence showing that MAPK pathways, including Jnk and p38 MAPK, are activated in PC3 cells treated with HVJ-E. Moreover, the

results from inhibitor treatments have further verified that inhibition of MAPK pathway reduces the HVJ-E-induced cytotoxic effects on PC3 cells. Together, these results reinforce the notion that the activation of MAPK pathway may perturb apoptosis in PC3 cells. To test the direct effect of HVJ-E on prostate cancer cell apoptosis *in vivo*, we excluded immunostimulatory effects in the current study by using T cell-deficient BALB/c nude mice. Indeed, intratumoral HVJ-E treatment presented robust direct anti-tumor activities on prostate cancer cells in this *in vivo* model, where most of the tumor growth was remarkably inhibited. Therefore, we postulate that HVJ-E plays an important and direct role in inducing apoptosis that leads to tumor killing.

In total, we have demonstrated that HVJ-E triggers apoptosis in human prostate cancer cells. We underscore the role of caspase cascade, especially the extrinsic pathway, in the induction of apoptosis in PC3 cells upon HVJ-E treatment. Moreover, both the JNK and p38 MAPK pathways contribute to HVJ-E induced apoptosis in PC3 cells, which provides novel insights into the mechanism of the anti-tumor effect of HVJ-E and throws a new light upon alternative therapeutic approaches for human cancers.

REFERENCES

1. Russo A, Espinoza CL, Caggia S, et al. A new jasmonic acid stereoisomeric derivative induces apoptosis via reactive oxygen species in human prostate cancer cells. Cancer letters, 2012; 326, 199-205.
2. Antonarakis ES, Carducci MA, and Eisenberger MA. Novel targeted therapeutics for metastatic castration-resistant prostate cancer. Cancer letters, 2010; 291, 1-13.
3. Matsushima-Miyagi T, Hatano K, Nomura M, et al. TRAIL and Noxa Are Selectively Upregulated in Prostate Cancer Cells Downstream of the RIG-I/MAVS Signaling Pathway by Nonreplicating Sendai Virus Particles. Clin Cancer Res, 2012; 18, 6271-83.
4. Liu TC and Kirn D. Gene therapy progress and prospects cancer: oncolytic viruses. Gene therapy, 2008; 15, 877-84.
5. Freeman AI, Zakay-Rones Z, Gomori JM, et al. Phase I/II trial of intravenous NDV-HUJ oncolytic virus in recurrent glioblastoma multiforme. Mol Ther, 2006; 13, 221-8.
6. Meng S, Zhou Z, Chen F, et al. Newcastle disease virus induces apoptosis in cisplatin-resistant human lung adenocarcinoma A549 cells in vitro and in vivo. Cancer letters, 2012; 317, 56-64.
7. Sinkovics JG and Horvath JC. Newcastle disease virus (NDV): brief history of its oncolytic strains. J Clin Virol, 2000; 16, 1-15.
8. Csatary LK, Moss RW, Beuth J, et al. Beneficial treatment of patients with advanced cancer using a Newcastle disease virus vaccine (MTH-68/H). Anticancer research, 1999; 19, 635-8.
9. Msaouel P, Iankov ID, Allen C, et al. Engineered measles virus as a novel oncolytic therapy against prostate cancer. The Prostate, 2009; 69, 82-91.
10. Kaneda Y. Virosome: a novel vector to enable multi-modal

strategies for cancer therapy. Advanced drug delivery reviews, 2012; 64, 730-8.

11. Kurooka M and Kaneda Y. Inactivated Sendai virus particles eradicate tumors by inducing immune responses through blocking regulatory T cells. Cancer research, 2007; 67, 227-36.

12. Fujihara A, Kurooka M, Miki T, et al. Intratumoral injection of inactivated Sendai virus particles elicits strong antitumor activity by enhancing local CXCL10 expression and systemic NK cell activation. Cancer Immunol Immunother, 2008; 57, 73-84.

13. Kaneda Y. A non-replicating oncolytic vector as a novel therapeutic tool against cancer. BMB reports, 2010; 43, 773-80.

14. Kawaguchi Y, Miyamoto Y, Inoue T, et al. Efficient eradication of hormone-resistant human prostate cancers by inactivated Sendai virus particle. International journal of cancer, 2009; 124, 2478-87.

15. Zhang Q, Wang Z, Yuan Y, et al. Immunoadjuvant effects of hemagglutinating virus of Japan envelope (HVJ-E) on the inactivated H9 subtype avian influenza virus vaccine. Veterinary immunology and immunopathology, 2011; 141, 116-23.

16. Bellei B, Flori E, Izzo E, et al. GSK3beta inhibition promotes melanogenesis in mouse B16 melanoma cells and normal human melanocytes. Cellular signalling, 2008; 20, 1750-61.

17. Karasic TB, Hei TK, and Ivanov VN. Disruption of IGF-1R signaling increases TRAIL-induced apoptosis: a new potential therapy for the treatment of melanoma. Experimental cell research, 1994-2007; 316.

18. Liu F and Gu J. Retinoic acid inducible gene-I, more than a virus sensor. Protein & cell, 2011; 2, 351-7.

19. Kato H, Takeuchi O, Sato S, et al. Differential roles of MDA5 and RIG-I helicases in the recognition of RNA viruses. Nature, 2006; 441, 101-5.

20. Juang SH, Wei SJ, Hung YM, et al. IFN-beta induces caspase-mediated apoptosis by disrupting mitochondria in human advanced stage colon cancer cell lines. J Interferon Cytokine Res, 2004; 24, 231-43.

21. Chawla-Sarkar M, Leaman DW, and Borden EC. Preferential induction of apoptosis by interferon (IFN)-beta compared with IFN-alpha2: correlation with TRAIL/Apo2L induction in melanoma cell lines. Clin Cancer Res, 2001; 7, 1821-31.

22. Li L, Zhang J, Jin B, et al. Nitric oxide upregulation of caspase-8 mRNA expression in lung endothelial cells: role of JAK2/STAT-1 signaling. Molecular and cellular biochemistry, 2007; 305, 71-7.

23. Bian J, Wang K, Kong X, et al. Caspase- and p38-MAPK-dependent induction of apoptosis in A549 lung cancer cells by Newcastle disease virus. Archives of virology, 2011; 156, 1335-44.

24. Breitbach CJ, Thorne SH, Bell JC, et al. Targeted and armed oncolytic poxviruses for cancer: the lead example of JX-594. Current pharmaceutical biotechnology, 2012; 13, 1768-72.

25. Yaacov B, Eliahoo E, Lazar I, et al. Selective oncolytic effect of an attenuated Newcastle disease virus (NDV-HUJ) in lung tumors. Cancer gene therapy, 2008; 15, 795-807.

26. Heinzerling L, Kunzi V, Oberholzer PA, et al. Oncolytic measles virus in cutaneous T-cell lymphomas mounts antitumor immune responses in vivo and targets interferon-resistant tumor cells. Blood, 2005; 106, 2287-94.

27. Matsuda M, Nimura K, Shimbo T, et al. Immunogene therapy using immunomodulating HVJ-E vector augments anti-tumor effects in murine malignant glioma. Journal of neuro-oncology, 2011; 103, 19-31.

28. Zhang Q, Yuan WF, Zhai GQ, et al. Inactivated Sendai Virus Suppresses Murine Melanoma Growth by Inducing Host Immune Responses and Down-regulating β-catenin Expression. Biomed Environ Sci, 2012; 25, 509-16.